Point-by-point responses to Reviewer

Responses to the Major Comment of the Reviewer RC1:

1. First, biospheric fluxes represent a major source of uncertainty. Photosynthetic uptake and ecosystem respiration are both large fluxes that partially cancel each other, and small errors in their representation can strongly affect inferred anthropogenic emissions. In a regional inversion framework, biospheric fluxes should ideally be jointly optimized, or at least rigorously evaluated. In the present study, however, no validation of the vegetation fluxes is provided. At a minimum, a sensitivity analysis of the emission estimates with respect to the net ecosystem exchange (NEE) would be necessary to assess the impact of biospheric flux uncertainties.

Response to question 1:

We highly appreciate the reviewer's valuable and constructive comments. The validation of vegetation flux simulations has been added and presented in Section 3 of the revised manuscript (**lines 257–271**).

Lines 257-271:

3 Validation of NEE simulated by WRF-GHG in the Pearl River Delta region

Comparison of monthly forward-simulated net ecosystem exchange (NEE) with observations at the SY station is shown in Figure 2. The annual mean simulated and observed NEE were 0.21 μmol m^{-2} s^{-1} and 0.18 μmol m^{-2} s^{-1}, respectively. The simulation reasonably reproduced the observed seasonal variability, with a correlation coefficient (R) of 0.68, a mean bias of −0.03 μmol m^{-2} s^{-1}, and a root mean square error (RMSE) of 0.20 μmol m^{-2} s^{-1}. This performance is better than that reported by Liu et al. (2015) at Qianyanzhou Station (bias of −0.86 μmol m^{-2} s^{-1}) and by Zhang et al. (2017) at Changbaishan Station (bias of −0.71 μmol m^{-2} s^{-1}).

During the non-growing season (November–December and January–March), the mean bias was 0.08 μmol m^{-2} s^{-1}. In contrast, during the peak growing season (April–October), the bias reached −0.11 μmol m^{-2} s^{-1}. This discrepancy may be attributed to the difficulty of the VPRM model in capturing changes in carbon sources and sinks associated with intense vegetation physiological activities and complex meteorological conditions during the peak growing season. Overall, these results indicate that the model captures the main temporal characteristics of regional biospheric carbon exchange.

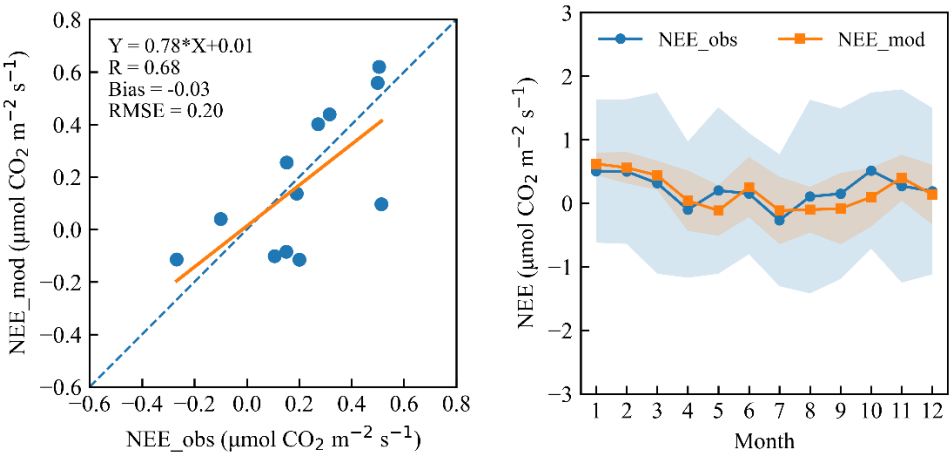

Figure 2. Comparison of monthly forward-simulated net ecosystem exchange (NEE_mod) and observed NEE (NEE_obs) at the SY station in the Pearl River Delta (PRD) region. The shaded areas represent one standard deviation.

2. Second, the treatment of background CO_2 concentrations is insufficiently constrained. While CarbonTracker products may exhibit small biases at large scales, their representation at regional scales is limited. In regional inversions, it is common practice to include an upwind background station and to simultaneously optimize background concentrations in order to avoid systematic biases in emission estimates arising from background errors. This aspect is not addressed in the current study.

Response to question 2:

We thank the reviewer for raising this important point. We fully agree that the representation of background CO_2 concentrations constitutes a major uncertainty source in regional atmospheric inversions, and we acknowledge that our current framework does not explicitly constrain background levels using independent upwind observations. Notably, the nested inner domains (d02 and d03) lack dedicated upwind background monitoring sites. In the absence of such *in situ* constraints, initial and lateral boundary conditions for all domains were derived from CarbonTracker outputs, a widely adopted approach in regional inversion modelling.

To partly address this limitation, the Jinsha National Atmospheric Background Station, situated within the outermost d01 domain, was used for independent model validation. The d01 domain provides lateral boundary constraints for the nested d02 and d03 domains. Validation against observations at the Jinsha site demonstrates that the posterior simulation considerably outperforms the prior simulation in reproducing ambient background CO_2 concentrations. The mean bias is

reduced from −7.71 ppm to −0.75 ppm, while the RMSE decreases from 13.51 ppm to 12.81 ppm. These results indicate that the inversion framework effectively improves the representation of regional and background CO_2 variability, even without dedicated optimization of background concentrations using separate upwind observations. **For the independent background validation at the JS station, please refer to lines 301-307 in the revised manuscript.**

Lines 301-307: For independent evaluation, we used continuous CO_2 records from the Jinsha background station, which was kept unassimilated throughout the inversion framework (Figure S5). The posterior simulation showed better agreement with the in-situ background observations than the prior simulation. The annual mean observed, prior-simulated, and posterior-simulated CO_2 concentrations were 432.17 ± 12.98 ppm, 424.46 ± 9.50 ppm, and 431.42 ± 13.65 ppm, respectively. At this independent background site, data assimilation reduced the mean bias from −7.71 ppm to −0.75 ppm and lowered the RMSE from 13.51 ppm to 12.81 ppm. These results suggest that the inversion better represents CO_2 variability at an independent site and partly corrects biases related to regional transport and background conditions.

3. Third, the assimilation of nighttime CO_2 observations (if performed) raises additional concerns. Nighttime boundary layer heights are often overestimated in atmospheric models, which can lead to systematic concentration biases. An evaluation of model performance with respect to boundary layer dynamics, particularly at night, would therefore be essential to assess the reliability of the inferred emissions.

   The systematic upward correction of a posteriori CO_2 concentrations found in the study could plausibly be attributed, at least in part, to one or a combination of these three factors. This issue requires a much more thorough investigation.

Response to question 3:

We thank the reviewer for these constructive comments. We fully agree that the assimilation of nighttime CO_2 observations requires careful evaluation of model performance in simulating nocturnal boundary layer dynamics, and that the systematic upward correction of a posteriori CO_2 concentrations could be influenced by multiple factors. We would like to clarify, however, that the systematic upward bias noted in our study refers to the forward (prior) simulation, not to the posterior CO_2 concentrations. After data assimilation, the posterior CO_2 concentrations do not

exhibit a persistent positive bias. The only exception is a specific overestimation observed in September, which is limited to that month.

To address the reviewer's concerns, we have carried out the following evaluations.

（1） Nighttime planetary **boundary layer height (PBLH) evaluation**

We validated the WRF-GHG simulated PBLH against ERA5 reanalysis separately for daytime and nighttime across the study period. The model shows reasonable skill in reproducing PBLH variations, with mean biases of 149.5 m (daytime) and 119.2 m (nighttime), and an overall mean bias of 135.8 m. The slightly smaller nighttime bias suggests that nocturnal PBLH overestimation is not severe in our simulation, reducing the likelihood that nighttime PBLH errors systematically bias the assimilated CO_2 concentrations.

(2) Examination **of three potential contributors to the September overestimation**

We have analyzed three factors: (i) background CO_2 concentrations, (ii) nighttime PBLH representation, (iii) biogenic fluxes, and (iv) anthropogenic emissions.

Biogenic fluxes: Forward-simulated NEE in September (-0.24 μmol m^{-2} s^{-1}) is comparable to that in August (-0.21 μmol m^{-2} s^{-1}) and does not show a unique peak that could explain the September CO_2 overestimation, although it is less negative than the October value (-0.42 μmol m^{-2} s^{-1}). The biogenic fluxes along cannot is not responsible for the overestimation.

Background CO_2: Independent validation at the JS background station shows that the posterior simulation reduces the mean bias from -7.71 ppm in the forward run to -0.75 ppm, indicating that background errors are not the dominant cause of the September overestimation.

PBLH: As noted, the nighttime PBLH bias is moderate and comparable to the daytime bias, and the model captures the seasonal cycle well. PBLH errors alone cannot explain the September-specific overestimation.

Anthropogenic emissions*:* The prior uncertainty of anthropogenic emissions is large (95 %, represented by spatially correlated random perturbations applied to the EDGAR v7.0 inventory). We therefore infer that remaining uncertainties in anthropogenic emissions are the most likely primary contributor to the September overestimation.

（3）More thorough investigation

We agree with the reviewer that this issue requires a more thorough investigation. In the revised manuscript, we have added four dedicated paragraphs (**lines 329–354**) discussing these four factors.

We believe these revisions address the reviewer's concerns and provide a more balanced and transparent assessment of the uncertainties in our inversion system.

4. The term "near real-time" in the title appears misleading, as the study presents a retrospective inversion for the year 2022 rather than an operational or low-latency system. While the framework may be suitable for near-real-time applications, this is not demonstrated in the current analysis.

Response to question 4:

We thank the reviewer for this careful observation. We agree that the term "near real-time" in the original title is indeed misleading, because the study presents a retrospective inversion for the year 2022 and does not demonstrate an operational low-latency system.

To avoid any misunderstanding, we have revised the title to **"High-resolution inversion of anthropogenic carbon emissions in the Pearl River Delta region based on the four-dimensional local ensemble transform Kalman filter"** and have removed the phrase "near real-time" from the title and throughout the manuscript (including the abstract and main text).

The revised title more accurately reflects the scope of the present work. We appreciate the reviewer's suggestion to improve the clarity and precision of our description.

5. Finally, several crucial methodological details are missing. Critical information about the observations (e.g., sampling heights, assimilated time periods, potential rejection thresholds) and about the inversion system itself (e.g., ensemble size, spatial correlation lengths, localization strategy or cut-off radii, and assumed observation error correlation structures) are not provided. These details are essential for evaluating and interpreting the results and must be included for the study to be reproducible and scientifically assessable.

Response to question 5:

We greatly appreciate the reviewer's comment.

1. The sampling heights are provided in Section 2.4.2 (CO_2 Concentration Observation Data), as detailed in **lines 216–220 and 235–237** of the revised manuscript.

Lines 216-220: Atmospheric CO_2 concentration observations were collected from seven high-precision monitoring stations across the PRD and one national atmospheric background station in Central China: Boluo (BL, 23.2° N, 114.3° E, 75.2 m), Dongguan (DG, 22.8° N, 114.2° E, 140.9 m), Kaiping (KP, 22.4° N, 112.7° E, 54.3 m), Nanhai (NH, 23.2° N, 113.0° E, 95.5 m), Shiyan (SY,

22.6° N, 113.9° E, 50.0 m), Xiangzhou (XZ, 22.2° N, 113.6° E, 64.0 m), Xichong (XC, 22.5° N, 114.5° E, 15.0 m), and Jinsha National Atmospheric Background Station (JS, 29.6° N, 114.2° E, 751.6 m).

Line 235-237: CO_2 flux measurements between the surface and the atmosphere were conducted from January to December 2022 at an observation height of 40 m, which captures the flux characteristics at the vegetation canopy–atmosphere interface.

2. Details regarding the assimilated time periods, potential rejection thresholds, ensemble size, spatial correlation lengths, localization strategy, cut-off radii, and assumed observation error correlation structures have all been provided in the revised manuscript. Please refer to lines 159–162, 180-187, and 190-196.

Lines 180-187: The assimilation experiment was performed for the entire year 2022, in which only atmospheric CO_2 concentrations were assimilated, while NEE fluxes were not constrained. The assimilation window in this study was set to 72 h. Within this window, 4D-LETKF performed a 120-h ensemble forecast with 20 members, outputting hourly results. The 20 ensemble members were generated by applying spatially correlated random perturbations to the anthropogenic CO_2 emissions, with an uncertainty of 95%, to represent the prior uncertainties of the Emission Database for Global Atmospheric Research (EDGAR v7.0) over the PRD region. The first 24 h served as model spin-up without data assimilation. For each subsequent hour, simulated background observations and observation innovations were calculated simultaneously, including during nighttime hours.

Lines 190-196： In this study, localization was applied to the observation error covariance matrix based on physical distance to avoid discontinuities in the analysis. The observation error was multiplied by the inverse of a Gaussian function, causing the influence of an observation on the analysis to decay gradually toward zero with increasing distance from the analysis location. The localization length scales were set to 36 km, 12 km, and 4 km for domains d01, d02, and d03, respectively (Mai et al., 2024). Although the Gaussian function has infinitely long tails, we truncated the tails to approximate the fifth-order piecewise rational function (Miyoshi et al., 2007).

Lines 159-162： The observation errors were assumed to be independent of each other. Therefore, the R is a diagonal matrix. Each diagonal component of R was calculated as the square of the sum of the instrumental error variance and the sampling error variance. The instrumental error was assumed to be 0.1 ppm, and the sampling error was 6.68 ppm (Mai et al., 2024).

Response to Minor / Technical Comments

6. **S2L45–50:** Consider citing ICON-ART applications for CO_2 simulations and inversions (e.g., Ponomarev et al., 2026). This reference is also relevant for S2L82–85, as it similarly addresses urban CO_2 emissions.

Response to question 6:

Done.

The recommended reference (Ponomarev et al., 2026) has been added to the Introduction section to further supplement recent advances in urban-scale CO_2 inversions. Please refer to lines 46–47.

Lines 46-47: Ponomarev et al. (2026) estimated CO_2 fluxes in the cities of Zurich and Paris using the ICON-ART CTDAS inverse modelling framework.

7. **S4L101:** A brief description of the 4D-LETKF method, its key features, and references to foundational studies (e.g., Hunt et al., Ott et al. Etc...) would help contextualize the methodology for readers unfamiliar with it.

Response to question 7:

Done.

A brief description of the 4D-LETKF method, including its key features, has been added to the **Introduction** in the revised manuscript. Please refer to lines 68–72.

Lines 68-72: The four-dimensional local ensemble transform Kalman filter (4D-LETKF) is a recently developed data assimilation technique (Hunt et al., 2007; Ott et al., 2004). Compared to 3D assimilation methods, 4D-LETKF offers computational efficiency for hourly updates and the ability to handle asynchronous observations (Dai et al., 2019a). It has demonstrated potential for the top-down inversion of atmospheric pollutant emissions (Dai et al., 2019b; 2021; Cheng et al., 2019), but its application to CO_2 emission inversion, especially in urban areas, has not yet been explored.

8. **S4L111:** The phrase "inverted CO_2 concentrations" is misleading. Emissions are inferred by the inversion, not the concentrations themselves. A more appropriate term would be *posterior* or *analyzed CO_2 concentrations*.

Response to question 8:

We thank the reviewer for pointing this out. The term "inverted CO_2 concentrations" has been replaced with "posterior CO_2 concentrations" to avoid misleading wording. Please refer to line 80.

Line 80: Section 3 presents the verification and analysis of posterior CO_2 concentrations across multiple spatiotemporal scales.

9. **S4L118**: Please **add** a reference for VPRM (e.g., Mahadevan et al., 2008).

Response to question 9:

Done.

10. **S7L179:** Clarify the definition of *xb* . It is the ensemble mean, not the emissions; EDGAR provides the prior from which the ensemble is drawn. Also specify whether the stated uncertainty corresponds to 1σ or 2σ.

Response to question 10:

We thank the reviewer for these constructive comments. The definition of $\bar{x}^b$ and stated uncertainty have been added to the revised manuscript. Please refer to line 149-150.

Lines 149-150: where $\bar{x}^b$ represents only the ensemble mean anthropogenic carbon emissions over d01, d02, and d03, which are derived from the 2019 yearly mean CO_2 emissions provided by EDGAR v7.0, with an associated 1σ uncertainty of 95%.

11. **S7L180:** The correlation length (and structure) used in the inversion should be stated explicitly.

Response to question 11:

Done. Please refer to line150-152 in the revised manuscript.

Lines 150-152: The background ensemble perturbation matrix is generated through spatiotemporal correlation perturbation, in other word, same random perturbation factors are used throughout the whole domain emission grids for each member.

12. S7L181: The description of *Xb* as a "matrix of each ensemble member" is unclear. Consider phrasing it as the ensemble perturbation matrix.

Response to question 12:

Done. Please refer to our response to Comment 10.

13. **S7L187:** Provide details on the observation error covariance *R*, including the magnitudes and the assumed correlation structure. How are they determined? Are they dependent on the prior concentrations or meteorological conditions?

Response to question 13:

Done. Please refer to **line 159-162** in the revised manuscript.

Lines 159-162: The observation errors were assumed to be independent of each other. Therefore, the R is a diagonal matrix. Each diagonal component of R was calculated as the square of the sum of the instrumental error variance and the sampling error variance. The instrumental error was

assumed to be 0.1 ppm, and the sampling error was 6.68 ppm (Mai et al., 2024).

14. **S7 Sect. 2.3:** Several methodological aspects remain unclear. For example, how and where was localization applied? Which observations were assimilated, including night-time measurements? What are the prior uncertainty correlation lengths and the observation error assumptions?

Response to question 14:

We thank the reviewer for these constructive comments. All the information has been given in the revised manuscript. Please refer to **lines 185-187 and lines 190-196**.

Lines 185-187: For each subsequent hour, simulated background observations and observation innovations were calculated simultaneously, including during nighttime hours.

Lines 190-196: In this study, localization was applied to the observation error covariance matrix based on physical distance to avoid discontinuities in the analysis. The observation error was multiplied by the inverse of a Gaussian function, causing the influence of an observation on the analysis to decay gradually toward zero with increasing distance from the analysis location. The localization length scales were set to 36 km, 12 km, and 4 km for domains d01, d02, and d03, respectively (Mai et al., 2024). Although the Gaussian function has infinitely long tails, we truncated the tails to approximate the fifth-order piecewise rational function (Miyoshi et al., 2007).

15. **S8L198–199:** The formulation is imprecise. Xa represents ensemble perturbations, not a state ensemble. The posterior ensemble members are reconstructed from $\bar{x}^a$ and Xa, not by simply adding $\bar{x}^a$ to Xa.

Response to question 15:

We thank the reviewer for this careful and insightful comment. We agree that the original statement was imprecise. To avoid potential misunderstanding, we have updated the corresponding description. Please refer to line 172 in the revised manuscript.

We apologize for this imprecise wording and greatly appreciate the reviewer's suggestion, which has helped improve the clarity of our presentation.

Line 172: In ensemble analysis, optimal anthropogenic carbon emission estimates are reconstructed from $\bar{x}^a$ and X^a.

16. S8L208**:** The term "observation biases" is likely intended to describe *residuals* or *innovations*. Consider clarifying this.

Response to question 16:

Done. Please refer to lines 185-187.

Lines 185-187: The first 24 h served as model spin-up without data assimilation. For each subsequent hour, simulated background observations and observation innovations were calculated simultaneously, including during nighttime hours.

17. **S9L230 ff.:** Provide the sampling height of the in-situ CO_2 observations, which is critical for interpreting results.

Response to question 17:

Done. Please refer to our response to Comment 5.

18. **S10L263:** Comparing posterior concentrations at in-situ stations with (prior) satellite XCO_2 is problematic. It's not an apples-to-apples comparison due to fundamentally different vertical sensitivities and averaging kernels. Please clarify the rationale.

Response to question 18:

We agree with the reviewer's comment. To avoid potential misunderstanding and overinterpretation, we have removed this statement from the revised manuscript.

19. **S9** Sect**. 3:** So far, the inversion period has not been explicitly stated. Please do so.

Response to question 19:

We appreciate the reviewer's comment. The inversion period has been added in the revised manuscript. Please refer to lines 180–181.

Lines 180-181: The assimilation experiment was performed for the entire year 2022, in which only atmospheric CO_2 concentrations were assimilated, while NEE fluxes were not constrained.

20. **S9 Sect. 3:** The analysis shows the inversion reproduces the assimilated observations better than the prior forward run (so what an inversion is supposed to do), but this is not a proper validation. Are there independent stations that could be used? Fit-to-obs validations, such as the chi-squared metrics, could help quantify fit quality.

Response to question 20:

We thank the reviewer for this constructive comment. We fully agree that the improved agreement of the inversion results with assimilated observations relative to the prior forward simulation is an inherent expected feature of any inversion framework and cannot serve as a rigorous independent validation. Since all available *in situ* CO_2 sites within the PRD domain were assimilated to impose optimal constraints on regional anthropogenic emissions, no additional independent observational sites remain inside the PRD for further validation.

Nevertheless, to address the reviewer's concern, we have incorporated two complementary quantitative evaluations into the revised manuscript:

First, chi-squared (χ^2) statistics are adopted to quantify the model–observation misfit across all assimilated stations. The domain-averaged χ^2 decreased from 3.21 for the prior run to 1.61 for the posterior run after data assimilation (**lines 296–300**), indicating a notable reduction in model–observation discrepancy. Although this metric does not constitute fully independent validation, it provides a more rigorous evaluation of consistency than a simple prior–posterior comparison.

Second, we perform independent validation using the Jinsha (JS) National Atmospheric Background Station. This site is located in the outer d01 domain and was not included in the assimilation network. At this independent background site, data assimilation reduced the mean bias from −7.71 ppm to −0.75 ppm and decreased the RMSE from 13.51 ppm to 12.81 ppm (**lines 301–307**). These results demonstrate that the inversion framework effectively reproduces CO_2 variability at a site outside the assimilation domain, offering a more robust assessment of overall inversion performance.

We believe these supplementary analyses adequately address the reviewer's concerns regarding model validation. Further details can be found in the revised manuscript.

21. **S10L267–268:** Strongly improved agreements with assimilated observations may reflect overfitting. Presenting chi-squared or fit-to-observation statistics would help assess the robustness of the inversion.

Response to question 21:

We thank the reviewer for raising the important issue of potential overfitting. We agree that strong improvement in agreement with assimilated observations alone does not guarantee robustness and may indicate overfitting. To address this concern, we have followed the reviewer's suggestion and added chi-squared (χ^2) statistics to quantify the fit quality across all assimilated stations (see our detailed response to **Comment 20**). The domain-averaged χ^2 decreased from 3.21 (prior) to 1.61 (posterior) after data assimilation, indicating a substantial reduction in model-observation misfit without evidence of overfitting (the posterior χ^2 remains above 1, suggesting that the inversion is not over-tuned to the observations). Furthermore, we conducted an independent validation using the Jinsha (JS) National Atmospheric Background Station, which was not assimilated. The posterior simulation reduced the mean bias from −7.71 ppm to −0.75 ppm and the RMSE from 13.51 ppm to 12.81 ppm at this independent site. These results collectively demonstrate that the inversion improves the representation of CO_2 variability without sacrificing

generalizability. We have added these analyses to the revised manuscript (**lines 296–307**). We are grateful to the reviewer for helping us strengthen the validation of our inversion system.

22. **S12L291:** The statement attributing discrepancies solely to underestimated EDGAR emissions may be oversimplified. Other factors, such as uncertainties in biospheric fluxes, background concentrations, or night-time boundary layer representation, should be tested and discussed (see my general comments).

Response to question 22:

We appreciate the reviewer's valuable comment. The uncertainties associated with biospheric fluxes, background concentrations, and nighttime boundary layer representation have been added to the revised manuscript. Please refer to **lines 329–336**.

Lines 329-336: The validation of forward-simulated NEE yielded a mean bias of −0.03 μmol m^{-2} s^{-1} (Figure 2). In addition, nighttime planetary boundary layer height (PBLH) from WRF-GHG simulations was evaluated against ERA5 reanalysis datasets (Figures S6–S8), with an overall mean bias of 119.2 m over the entire study period. The above results indicated that WRF-GHG reasonably reproduced biogenic fluxes and nighttime PBLH across the PRD region, implying that these two factors were not responsible for the low bias in the forward simulation. Considering the forward-simulated CO_2 deviation of −7.71 ppm at the JS background station (Figure S5) and the substantial underestimation inherent in the EDGAR v7.0 emission inventory, these two factors were likely the dominant contributors to the model bias.

23. **S13L304:** Correct terminology: *time series* rather than *distributions*.

Response to question 23:

Done.

24. **S13** Fig**. 6:** The inversion reproduces the assimilated observations, but it is unclear how this compares to observational uncertainties. Possible overfitting should be discussed; again, independent validation or chi-squared metrics would be informative.

Response to question 24:

We fully agree with this constructive comment. To quantitatively assess model performance and rule out potential overfitting, we have adopted chi-squared(χ^2) statistics to quantify the model-observation misfit for all assimilated sites. Meanwhile, we have supplemented independent validation results based on monthly CO_2 records from the JS background station, which can

effectively reflect the inversion performance beyond the assimilation domain. Relevant analyses have been added in the revised manuscript **(lines 358–363)**.

Lines 358–363： The chi-squared (χ^2) statistics for hourly CO_2 concentration validation at all assimilated stations in the PRD region show that the domain-averaged χ^2 decreased from 3.21 (prior) to 1.61 (posterior) after data assimilation, indicating a notable reduction in model-observation misfit with no sign of overfitting (Table S1). To further verify the reliability of the inversion results, we conducted independent validation using monthly CO_2 concentrations observed at the JS background station (Figure S5(c)). The annual mean bias dropped from −8.03 ppm in the prior simulation to −0.85 ppm in the posterior simulation.

25. **S14L330:** Especially the influence of misrepresented nocturnal PBL height could be large and contribute to systematic biases.

Response to question 25:

We fully agree with the reviewer's comments. We have validated diurnal PBLH simulated by WRF-GHG against ERA5 reanalysis data in the revised manuscript. The results confirm that the model can reasonably capture the diurnal evolution of regional PBLH. During rush hours, the mean PBLH biases reach 82.23 m at the BL site and 118.26 m averaged across all stations. Relevant content is presented in **lines 392–394**.

Lines 392-394: Diurnal PBLH from WRF-GHG was validated against ERA5 reanalysis data (Figure S9). The results demonstrate that the model satisfactorily reflect rush-hour variations in regional PBLH, with mean biases of 82.23 m at the BL station and 118.26 m across all stations.

26. **S17 Fig. 9b:** Increase the figure size. Inversion-EDGAR maps are particularly important, as they reflect actual emission innovations. Please indicate station locations on the maps.

Response to question 26:

Done

27. **S17 Fig.** 9b**:** Inversion-Edgar: Why do we see the pattern where upward adjustments are surrounded by downward adjustments?

Response to question 27:

We sincerely apologize for the plotting error in Figure 9b in the original manuscript. The abnormal spatial pattern featuring upward adjustments surrounded by downward ones originated from plotting mistakes, rather than inherent errors in the inversion outputs. We have thoroughly checked the raw data and fully revised this figure accordingly (Figure 10 in the revised manuscript).

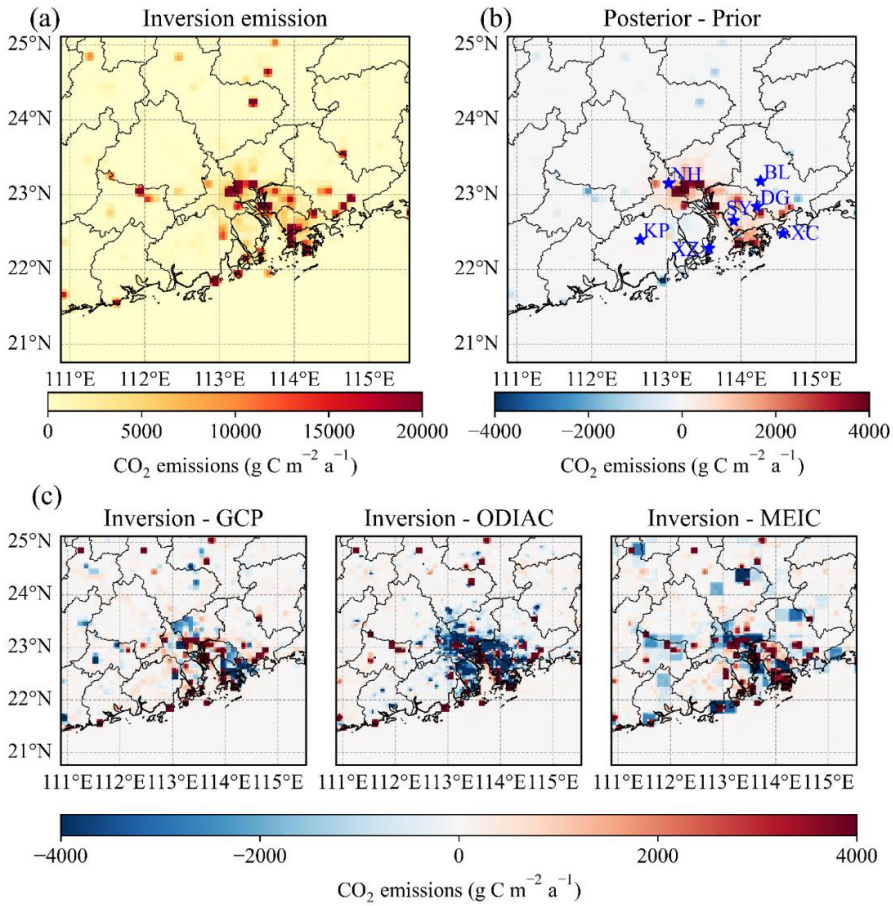

Figure 10. Spatial distribution of the anthropogenic CO_2 inversion inventory and their differences compared to bottom-up inventories in the Pearl River Delta (PRD) region in 2022. (a) Anthropogenic CO_2 inversion inventory obtained in this study; (b) spatial differences between the inversion inventory and the prior inventory (EDGAR v7.0); (c) spatial differences between the inversion inventory and three bottom-up statistical inventories (GCP, ODIAC, and MEIC).The blue stars denote observational sites. NH: Nanhai Station; KP: Kaiping Station; XZ: Xiangzhou Station; SY: Shiyan Station; DG: Dongguan Station; BL: Boluo Station; XC: Xichong Station.

28. **S17** and **all other figures:** Please use perceptually uniform colormaps.

Response to question 28:

We appreciate this valuable suggestion. We have replaced the original color scheme with perceptually uniform colormaps for all spatial plots in the revised manuscript, which can effectively ensure consistent visual perception of gradient variations and improve the readability and scientific presentation of our figures.

29. **S19 Fig. 11 and S22 Fig. 13a:** Displaying sectoral emission contributions (traffic, energy, industry) would help interpret seasonal and diurnal emission patterns. Their discussion would strengthen the interpretation of the results.

Response to question 29:

We sincerely appreciate the reviewer's constructive and insightful comment. We fully acknowledge that presenting sector-level emission contributions (e.g., traffic, energy and industry) would greatly facilitate the interpretation of seasonal and diurnal emission characteristics. Nevertheless, our inversion framework is designed to constrain total anthropogenic CO_2 emissions and cannot directly separate sector-specific emission fluxes.

To mitigate this limitation, we have supplemented relevant sectoral analyses in the revised manuscript based on the monthly EDGAR v8.0 emission inventory and other bottom-up datasets including ODIAC, GCP GridFED and MEIC. Specifically, we illustrate the seasonal contributions of key sectors (power, industry and transportation) derived from these inventories in the newly added Figure 12 and Figure S10, together with corresponding discussions **(lines 517–552** in the revised manuscript), to better explain the seasonal variations obtained by our inversion results.

We further discuss the potential links between such sectoral emission distributions and diurnal emission features (**lines 587–597**). Given that our inversion cannot directly retrieve sectoral emissions, the relevant analysis remains partially qualitative. We believe these supplementary analyses substantially improve the scientific interpretation of our findings. Detailed information can be found in the revised manuscript.

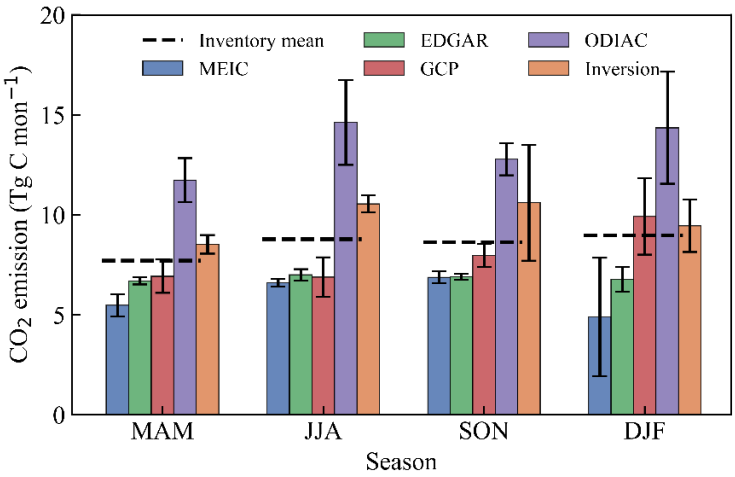

Figure 12. Seasonal variations of anthropogenic CO_2 emissions over the Pearl River Delta (PRD) in 2022, derived from the inversion results and four bottom-up inventories (EDGAR v8.0, ODIAC, GCP, and MEIC). MAM, JJA, SON, and DJF denote March–May, June–August, September–November, and December–February, respectively. The dashed line indicates the mean of the four bottom-up inventories. "Inversion" refers to the emission estimates from the top-down inversion.

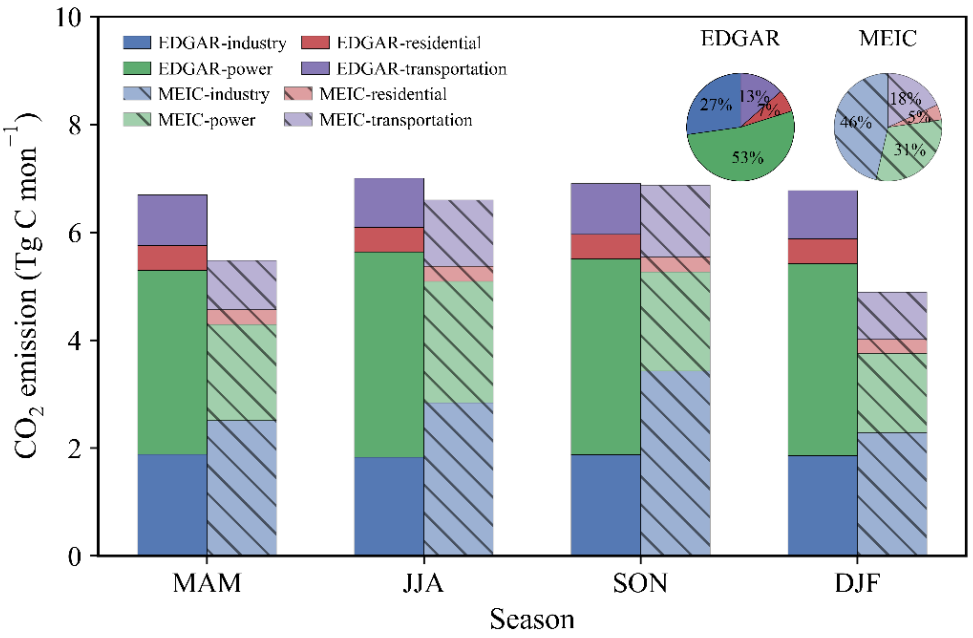

Figure S10. Seasonal comparison of sectoral anthropogenic CO_2 emissions from the EDGAR and MEIC inventories over the Pearl River Delta (PRD) in 2022. Stacked bars denote seasonal emissions from the industrial, power, residential and transportation sectors, while the inset pie charts summarise the annual fractional contribution of each sector to total regional emissions for both EDGAR and MEIC.

30. **S22L515:** In addition, the winter monsoon transports air from inland regions that has already been influenced by emissions. It's not only the higher CO2 concentrations of the air coming from higher latitudes.

Response to question 30:

We agree with this comment. We have revised the relevant descriptions accordingly, as detailed in lines **635–637** of the revised manuscript.

Lines 635-637: Additionally, driven by winter monsoon winds, air masses transported from inland regions that had already been influenced by upstream anthropogenic emissions further increased CO_2 concentrations in the PRD region (Figure S12).

31. **Results section (general):** Some descriptions of individual numerical values are lengthy but add little value beyond the figures. Consider condensing the text and focusing on interpretation and key insights.

Response to question 31:

We fully agree with this comment. We have streamlined redundant numerical descriptions throughout the revised text, removed lengthy trivial value statements, and concentrated more on result interpretation and key scientific implications.